

New perylenes for dye sensitization of TiO₂

Suzanne Ferrere* and Brian A. Gregg

Basic Sciences Center, National Renewable Energy Laboratory, 1617 Cole Blvd., Golden, CO 80401, USA

Received (in New Haven, CT, USA) 14th December 2001, Accepted 24th March 2002

First published as an Advance Article on the web 30th July 2002

We describe a new generation of perylene photosensitizers based upon *N*-(2,5-di-*tert*-butylphenyl)perylene-3,4-dicarboximide. The new sensitizers have more favorable energetics for electron injection into TiO₂ and better light absorption properties for solar conversion than previous sensitizers based upon perylene tetracarboxylic acid dianhydride. Syntheses, absorption properties, and electrochemical potentials for the new perylenes are reported. We compare the solar conversion efficiencies of the dyes in the dye sensitized solar cell (DSSC) and discuss trends in terms of energetics and structural differences that may affect the injection and recombination processes. These are the highest efficiencies yet reported for perylene sensitizers in the DSSC.

The dye sensitized solar cell (DSSC) utilizes adsorbed dye molecules to sensitize nanocrystalline particles of the large bandgap semiconductor titanium dioxide (TiO₂) to the visible portion of the solar emission spectrum.^{1,2} The primary process is similar to photographic sensitization, in which the dye absorbs light and its photoexcited state injects an electron into the TiO₂ conduction band. The highest efficiency DSSC device contains the “N3” dye, [Ru(4,4'-dicarboxy-2,2'-bipyridine)₂(NCS)₂], and most fundamental studies also employ this sensitizer.^{3–7} However, questions remain about the long term stability and cost issues of metal bipyridyl sensitizers in a commercial application. Although organic molecules are generally less expensive, have better optical properties, and have a longer history of commercial use as sensitizers and dyes, the efficiencies for DSSC's containing organic photosensitizers have lagged behind the efficiencies of DSSC's with metal bipyridyl sensitizers. However, there appears to be no fundamental limitation to obtaining a high efficiency DSSC with an organic dye.

Perylene diimides are robust, thermally stable and inexpensive organic molecules that are used as commercial pigments and vat dyes.^{8,9} These properties, in addition to their excellent photophysical properties (large molar absorption coefficients and fluorescence yields), make perylenes ideal for light-based applications. Accordingly, perylene diimide films have been used as photoreceptors in xerographic devices and n-type semiconductor components in organic solar cells.^{10,11} In 1997 we showed that perylene tetracarboxylic acid dianhydride (PTCDA) and dyes derived from it, like perylene-3,4-dicarboxylic acid anhydride-*N*-(dodecyl)-9,10-carboximide (P4 in Table 1), could be used as chromophores in the DSSC.¹² However, although they were efficient sensitizers of nanocrystalline SnO₂, they were poor sensitizers of TiO₂. These results could be explained by differences in energetics between the two semiconductors: electron injection had 500 mV more driving force for SnO₂ than for TiO₂ because of the relative positions of their conduction bands. In addition, the PTCDA-based sensitizers did not have optimum light absorption properties for solar conversion, and suffered from practical problems such as poor solubility and aggregation.

In recent years, Langhals and coworkers have introduced a variety of synthetic strategies for preparing perylene dyes with improved solution properties.^{13,14} By expanding upon

Langhals's methods, we have synthesized new perylene sensitizers with better solubilities, more negative excited state energies, and better visible light absorption properties for solar conversion. The new perylene dyes are excellent sensitizers of TiO₂. Here we report syntheses for the new dyes, present their sensitization behavior and trends, and compare them with our previous perylene sensitizers and with the more widely used metal bipyridyl systems.

Experimental

Materials and methods

All reagents were of commercial grade and used as received unless otherwise specified. Perylene-3,4,9,10-tetracarboxylic dianhydride (PTCDA) was obtained from Aldrich. Perylene-3,4-dicarboxylic anhydride-*N*-(dodecyl)-9,10-carboximide (P4 in Table 1) was prepared by the reaction of monopotassium 3,4 : 9,10-perylene tetracarboxylate with dodecylamine.¹² It should be noted that the NMR signals for the perylenes were observed to shift with their concentration in the deuterated solvent, presumably due to the effects of aggregation on ring protons. Mass spectrometry analysis was provided by the Central Analytical Laboratory at the Department of Chemistry and Biochemistry, University of Colorado at Boulder. Electron ionization (EI) spectra were obtained from a direct probe at 70 eV and 1500 resolution using a Micromass AutoSpec M mass spectrometer. Liquid secondary ion mass spectrometry (LSI-MS) was performed from the matrix *m*-nitrobenzyl alcohol using the same instrument. Electrospray ionization (ESI) mass spectra were obtained using an HP 5989B ESI mass spectrometer. Nanocrystalline TiO₂ films were prepared and assembled into DSSC's as previously reported.^{15,16} Films were typically 4–6 μm thick. Assembled cells were treated with ultraviolet (UV) light to maximize their efficiency.¹⁷ Incident-photon-to-current efficiency (IPCE) spectra and current-voltage (*J-V*) measurements were generated using LabVIEW programs written for Macintosh. The cells were illuminated through the TiO₂ electrode with monochromatic light or the full spectrum (> 400 nm) from a Xenon arc lamp (PTI, model A 1010) for IPCE and *J-V* measurements, respectively. The current was monitored by a Keithley 236 source measure unit.

Table 1 Electrochemical oxidation potentials in solution and absorption maxima in solution and as adsorbed. For adsorbed spectra, films were wetted with methoxypropionitrile and measured *vs.* air

Dye	Structure	$E_{1/2}^a/V$ vs. Fc	$\lambda_{\text{MAX}}/\text{nm}$ (sol)	$\lambda_{\text{MAX}}(\text{ads})/\text{nm}$
P1		+0.49	556 (CH ₃ CN)	< 480
P2		+0.42	560 (CH ₃ CN)	452
P3		+0.53	500 (CH ₃ CN) 550 (CH ₂ Cl ₂)	531
P4		$\sim +0.89^{12}$	509 (NMP)	486
P5		+0.59	506 (CH ₂ Cl ₂)	500
P6		+0.71	485 (CH ₂ Cl ₂)	–

^a Measured in methylene chloride.

“One sun” (AM 1.5) calibration was performed as previously described.¹⁷

Preparation of dyes

P6 and derivatives. *N*-(2,5-Di-*tert*-butylphenyl)perylene-3,4-dicarboximide (**P6**) was prepared according to the method of Langhals *et al.*,¹⁴ but using 6.04 g perylene-3,4,9,10-tetracarboxylic dianhydride, 30.86 g imidazole, 2.18 g zinc acetate dihydrate, 13.2 mL deionized water, and 1.73 g di-*tert*-butylaniline. The reactants were placed in a 165 mL titanium autoclave fitted with a teflon insert and heated at 190 °C for 23 h. After separation on silica gel using chloroform as eluent, the product was recrystallized from ethyl acetate.

9-Bromo-*N*-(2,5-di-*tert*-butylphenyl)perylene-3,4-dicarboximide and 9-amino-*N*-(2,5-di-*tert*-butylphenyl)perylene-3,4-dicarboximide (**3**) were also prepared according to Langhals¹⁴ and recrystallized from ethyl acetate. Yields were similar to literature values.¹⁴

2. 9-Dioctylamino-*N*-(2,5-di-*tert*-butylphenyl)perylene-3,4-dicarboximide (**2**) was prepared by reacting 9-bromo-*N*-(2,5-di-*tert*-butylphenyl)perylene-3,4-dicarboximide (**1**, 422 mg, 0.717 mmol) with dioctylamine (2.0 g, 8.3 mmol) in 5 mL dimethylformamide (DMF). The reaction was carried out in a 100 mL round bottomed flask and refluxed overnight under an argon flow, yielding a purple solution. The DMF was removed on a rotary evaporator and the reaction mixture was dried in a vacuum oven at 80 °C. Chromatography on silica gel with chloroform as eluent yielded the product as a prominent purple band in yields ranging from $\sim 10\%$ to $\sim 35\%$. NMR (CDCl₃) 8.62 ppm (t, 1H, $J = 8.1$ Hz); 8.61 (d, 1H, $J = 8.1$ Hz);

8.48 (d, 1H, $J = 8.1$ Hz); 8.43, 8.4, 8.33, 8.31 (all d, 1H each, $J = 8.1$ Hz); 7.65 (d, 1H, $J = 8.1$ Hz); 7.58 (d, 1H, $J = 8.1$ Hz); 7.44 (dd, 1H, $J = 8.1$, < 3 Hz); 7.23 (d buried under CHCl₃ signal, 1H); 7.03 (d, 1H, $J < 3$ Hz); 3.28 (t, 4H, $J = 7.8$ Hz); 1.56 (m, 4H); 1.33 (s, 9H); 1.30 (s, 9H); 1.23 (m, 20H); 0.7 (t, 6H, $J = 7.8$ Hz).

P2. 9-Dioctylaminoperylene-3,4-dicarboxylic acid anhydride (**P2**) was prepared according to Wasielewski *et al.* by reacting 9-dioctylamino-*N*-(2,5-di-*tert*-butylphenyl)perylene-3,4-dicarboximide (approximately 749 mg as a residue, 1 mmol) with 2.74 g (49 mmol) KOH in 65 mL 2-methyl-2-propanol in a 100 mL round bottomed flask and refluxing for 1.5 h.¹⁸ After cooling, the reaction mix was added to ~ 130 mL glacial acetic acid and stirred in a 500 mL beaker overnight. The product did not precipitate, so the solution was rotary evaporated to dryness and re-suspended in water by immersing the flask in an ultrasonic bath. The purple solid was collected on a 0.45 μm nylon filter paper and rinsed with deionized water, then vacuum dried at 80 °C. The product was isolated by column chromatography (silica gel, 1 : 1 CHCl₃–methanol), eluting as the second band. Yield 50%. UV-VIS $\lambda_{\text{max}} = 560$ nm (CH₃CN); NMR (CDCl₃) δ 8.36 (t, 2H, $J = 8.1$ Hz); 8.35 (d, 1H, $J = 5.4$ Hz); 8.28 (t, 2H, $J = 8.1$ Hz); 8.19 (d, 1H, $J = 6.9$ Hz); 8.09 (d, 1H, $J = 6.9$ Hz); 7.61 (t, 1H, $J = 8.1$ Hz); 7.2 (d, 1H, $J = 8.1$ Hz); 3.32 (t, 4H, $J = 5.4$ Hz); 1.62 (br t, 4H); 1.25 (m, 20H); 0.7 (t, 6H, $J = 5.4$ Hz). MS: m/z (%) 561 (100) [M⁺], 462 (94), 350 (25), 418 (10), 277 (15).

P3. 9-Dioctylamino-*N*-(acetic acid)perylene-3,4-dicarboximide (**P3**) was prepared by adding 128.7 mg (2.29 mmol) KOH and 171.9 mg (2.29 mmol) glycine, dissolved in 5 mL

deionized water, to 30 mg (0.053 mmol) of 9-dioctylaminoperylene-3,4-dicarboxylic acid anhydride in ~3 mL DMF. A precipitate formed when the two solutions were mixed but redissolved when 3 mL of additional DMF were added. The 100 mL round bottomed flask containing the reactants was heated in a 100 °C oil bath overnight. The reaction mixture was rotary evaporated to dryness, then dissolved in CHCl₃–CH₃OH (8 : 2) and filtered through a cotton plug to collect excess salt. The filtered solution was rotary evaporated to dryness, then re-dissolved in CHCl₃. Isolation of the product was achieved on silica gel by gradient elution of methanol (2% to 100% by volume) in CHCl₃. The purified product was evaporated to dryness and the residue was treated with 1 M HCl, rinsed with deionized water, then extracted into CH₂Cl₂ and back-extracted with 0.01 M HCl. The CH₂Cl₂ was evaporated and the product vacuum dried. Since it was collected as a residue the exact yield was not determined; however, it was estimated at ~60%. UV-VIS $\lambda_{\text{max}} = 550$ nm (CH₂Cl₂); NMR (CDCl₃) δ 8.41 (d, 2H, $J = 7.5$ Hz); 8.33 (d, 2H, $J = 7.5$ Hz); 8.28 (d, 1H, $J = 7.5$ Hz); 8.15 (t, 2H, $J = 9.3$ Hz); 7.61 (t, 1H, $J = 9.3$ Hz); 7.22 (d, 1H, $J = 7.5$ Hz); 5.0 (s, 2H); 3.33 (br t, 4H); 1.6 (br t, 4H); 1.25 (m, 20H); 0.65 (t, 6H, $J = 7.5$ Hz). MS: m/z (%) 663 (100) [MH⁺], 641 (69), 619 (50), 596 (18), 573 (47), 561 (12).

Precursor to P1. 9-Dimethylamino-*N*-(2,5-di-*tert*-butylphenyl)perylene-3,4-dicarboximide¹⁴ was obtained while attempting to prepare 9-aminodi(ethyl methylacetate)-*N*-(2,5-di-*tert*-butylphenyl)perylene-3,4-dicarboximide as follows: 327.6 mg (0.557 mmol) of 9-bromo-*N*-(2,5-di-*tert*-butylphenyl)perylene-3,4-dicarboximide were mixed with 2.4 mL (12.9 mmol) diethyl iminodiacetate in 8 mL DMF in a 100 mL round bottomed flask. It was refluxed for 48 h. The DMF was rotary evaporated from the purple reaction mixture, and the leftover diethyl iminodiacetate was dissolved in water, allowing the product to collect on a cotton filter. It was further rinsed with an additional 250 mL deionized water and vacuum dried at 80 °C. The reaction mixture was separated on silica gel using CHCl₃ eluent, and a purple product eluted as the first band. NMR revealed it to be 9-dimethylamino-*N*-(2,5-di-*tert*-butylphenyl)perylene-3,4-dicarboximide. The desired product of this reaction, 9-aminodi(ethyl methylacetate)-*N*-(2,5-di-*tert*-butylphenyl)perylene-3,4-dicarboximide, was not obtained. NMR (CDCl₃) δ 8.62 (dd, 2 H, $J = 7.8$, <1.5 Hz); 8.5 (d, 1H, $J = 7.8$ Hz); 8.42 (dd, 2H, $J = 7.8$, <1.5 Hz); 8.34 (d, 1H, $J = 7.8$ Hz); 8.29 (d, 1H, $J = 7.8$ Hz); 7.65 (t, 1H, $J = 7.8$ Hz); 7.58 (d, 1H, $J = 7.8$ Hz); 7.44 (dd, 1H, $J = 7.8$, 3 Hz); 7.19 (d, 1H, $J = 7.8$ Hz); 7.02 (d, 1H, $J = 3$ Hz); 3.05 (s, 6H); 1.33 (s, 9H); 1.3 (s, 9H).

P1. The dye 9-dimethylaminoperylene-3,4-dicarboxylic acid anhydride (**P1**) was obtained by hydrolyzing the *tert*-butylphenyl group from 9-dimethylamino-*N*-(2,5-di-*tert*-butylphenyl)perylene-3,4-dicarboximide in the manner described above for 9-dioctylaminoperylene-3,4-dicarboxylic acid anhydride.

P5. 9-Aminomethyl carboxylic acid-*N*-(2,5-di-*tert*-butylphenyl)perylene-3,4-dicarboximide (**P5**) was prepared by reacting 24 mg (0.048 mmoles) of 9-amino-*N*-(2,5-di-*tert*-butylphenyl)perylene-3,4-dicarboximide (**3**) with bromoacetic acid (181 mg, 1.3 mmoles) in 5 mL benzonitrile containing 25 mg (0.30 mmoles) sodium bicarbonate. Dilute tetra-*n*-butylammonium hydroxide (TBAOH) was added and the reaction mixture was rotary evaporated to dryness. It was then re-dissolved in chloroform and extracted with water; the chloroform layer was evaporated and dried under vacuum at 80 °C. Separation on silica gel with 10% ethyl acetate in chloroform yielded the TBA⁺ salt of the product, which was protonated by the addition of dilute (0.01 M) HCl. NMR (CDCl₃) δ 8.85 (s, 1H); 8.65

(d, 2H, $J = 8.7$ Hz); 8.39–8.53 (m, 4H); 8.23 (d, 1H, $J = 8.7$ Hz); 7.94 (d, 1H, $J = 8.7$ Hz); 7.74 (t, 1H, $J = 8.7$ Hz); 7.58 (d, 1H, $J = 8.7$ Hz); 7.45 (dd, 1H, $J = 8.7$, <3 Hz); 7.4 (s, 1H); 4.24 (s, 2H); 1.33 (s, 1H); 1.29 (s, 1H).

P4. Perylene-3,4-dicarboxylic acid anhydride-9,10-dodecylcarboximide (**P4**) was prepared according to procedure 2 in ref. 12.

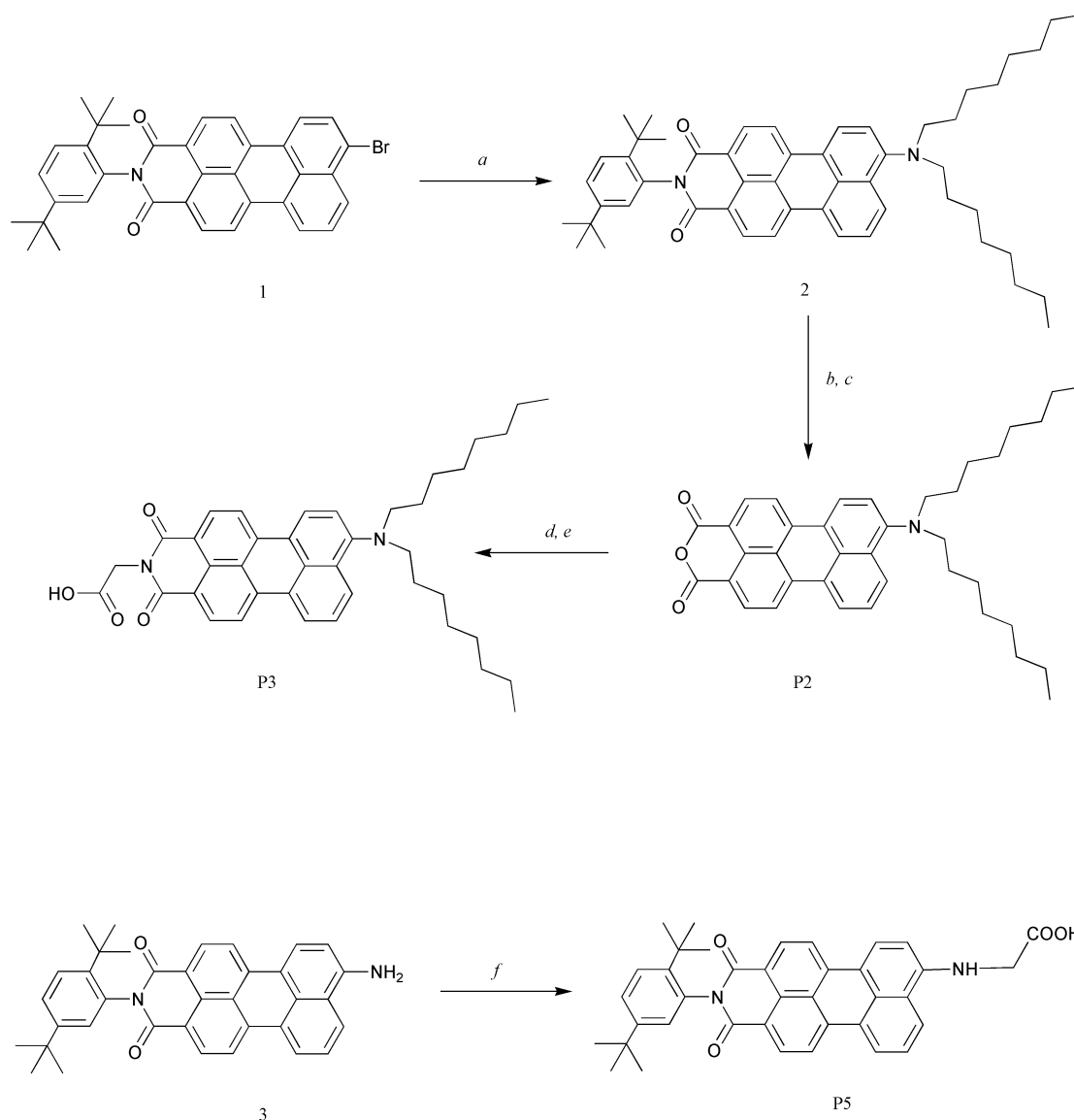
Results

Syntheses and solution properties

The synthetic pathways to **P2**, **P3**, and **P5** are illustrated in Scheme 1. We followed Langhals' procedure to prepare *N*-(2,5-di-*tert*-butylphenyl)perylene-3,4-dicarboximide (**P6**, Table 1) by a decarboxylating condensation of PTCDA with 2,5-di-*tert*-butylaniline.¹⁴ The di-*tert*-butylphenyl substituent prevents ring stacking and thereby improves the solubility and hinders aggregation. The perylene ring can be selectively brominated or nitrated, providing the starting materials 9-bromo-*N*-(2,5-di-*tert*-butylphenyl)perylene-3,4-dicarboximide (**1**) and 9-nitro-*N*-(2,5-di-*tert*-butylphenyl)perylene-3,4-dicarboximide, the precursor to 9-amino-*N*-(2,5-di-*tert*-butylphenyl)perylene-3,4-dicarboximide (**3**).¹⁴

It was anticipated that reacting **1** with alkylamines would be a straightforward route to 9-alkylamino-*N*-(2,5-di-*tert*-butylphenyl)perylene-3,4-dicarboximides. However, although we could prepare 9-dioctylamino-*N*-(2,5-di-*tert*-butylphenyl)perylene-3,4-dicarboximide (**2**) from **1** and dioctylamine, the yield was fairly low and there were many byproducts. All attempts to prepare other 9-dialkylamino or 9-monoalkylamino derivatives *via* the same route, employing amines that included iminodiacetic acid, diethyl iminodiacetate, 2,5-di-*tert*-butylaniline, aminomethylphosphonic acid and glycine, were unsuccessful. In each case there were multiple products, including quatterylene species,¹⁹ but very little, or none, of the desired product. The reaction employing diethyl iminodiacetate generated 9-dimethylamino-*N*-(2,5-di-*tert*-butylphenyl)perylene-3,4-dicarboximide, which turned out to be a useful byproduct and precursor to **P1**. The converse approach, reacting 9-amino-*N*-(2,5-di-*tert*-butylphenyl)perylene-3,4-dicarboximide (**3**) with bromoacetic acid, proved a successful route to 9-aminomethyl carboxylic acid-*N*-(2,5-di-*tert*-butylphenyl)perylene-3,4-dicarboximide (**P5**). However, the powders of both 9-dimethylamino-*N*-(2,5-di-*tert*-butylphenyl)perylene-3,4-dicarboximide and **P5** decomposed over time, yielding 9-methylamino-*N*-(2,5-di-*tert*-butylphenyl)perylene-3,4-dicarboximide and 9-aminoethyl-*N*-(2,5-di-*tert*-butylphenyl)perylene-3,4-dicarboximide, respectively. The decomposition products were confirmed by mass spectral analysis of the aged powders. Furthermore, it was observed that aged **P5** no longer adsorbed out of solution onto TiO₂ films (indicative of loss of the –COOH adsorbing group).

Absorption maxima for the π – π^* transition and electrochemical potentials for the oxidation process (Per/Per⁺) are shown in Table 1. All of the 9-alkylamino substituted perylene-3,4-dicarboximides have absorption maxima that are lower in energy than that of *N*-(2,5-di-*tert*-butylphenyl)perylene-3,4-dicarboximide (**P6**), due to the electron-donating effect of amino substitution; their solvatochromism also indicates strong charge transfer character. The *mono*alkylamino substituted dye **P5** has an absorption maximum (506 nm in dichloromethane) that is intermediate between the unsubstituted analog (485 nm) and the *dialkyl*amino substituted **P3** (550 nm). The nature of substitution is reflected similarly in their electrochemical potentials: **P3** is easier to oxidize than **P5**, which is easier to oxidize than **P6**. Approximate values



Scheme 1 (a) Dioctylamine, refluxing DMF; (b) KOH, 2-methyl-2-propanol; (c) acetic acid; (d) $\text{H}_2\text{NCH}_2\text{CO}_2\text{K}$, water, DMF, 100°C ; (e) HCl; (f) $\text{BrCH}_2\text{CO}_2\text{H}$, benzonitrile, sodium bicarbonate.

for the excited state oxidation potential of the dyes, calculated from $E_{1/2} - E_{0,0}$ in solution, are included in Table 2. For **P4**, its oxidation potential was estimated at $+0.89\text{ V vs. ferrocene}$.¹²

Adsorption onto nanocrystalline TiO_2

All of the dyes had good solubility in solvents such as acetonitrile, chloroform and dichloromethane, with the exception of **P4**, which was only slightly soluble in *n*-methylpyrrolidinone

Table 2 Approximate excited state oxidation potentials, calculated from solution emission spectra and $E_{1/2}$ values from Table 1, and average IPCE values from two DSSC measurements. Since **P1** and **P2** adsorb as carboxylates rather than as anhydrides, their effective potential is more negative than what is indicated here

Dye	E^*/V vs. Fc	Ave. IPCE max/%
P1	< -1.50	35.3
P2	< -1.49	66.5
P3	-1.43	26.0
P4	~ -1.46	20.0
P5	-1.69	39.0
N3	-1.21	67.5

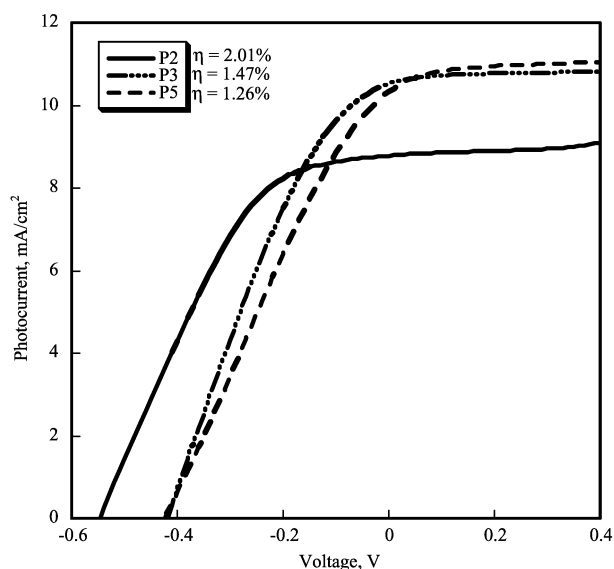
(NMP). Dark dyed films ($A_{\text{max}} > 2$) of TiO_2 were obtained from all dye solutions, including an NMP solution of **P4**. No emission was observed from the dyed films, with the exception of **P4**, which was still emissive in its adsorbed form. Absorption maxima for the *adsorbed* dyes are tabulated in Table 1; most of the dyes exhibit only slight shifts in their spectra upon adsorption onto TiO_2 . Like **N3** and related sensitizers, the perylenes adsorb onto the surface *via* their carboxylic acid groups. For **P1** and **P2**, large shifts in absorption maxima ($\sim 100\text{ nm}$, Table 1) indicate that the anhydride ring opens and the dyes bind to the TiO_2 surface in the dicarboxy form. This is confirmed by the adsorbed spectra's resemblance to the solution spectra of **P1** and **P2** as deprotonated TBA^+ salts. The TBA^+ forms have a more negative reduction potential than the anhydride form in solution, and adsorption likely perturbs the excited state energetics of **P1** and **P2** analogously.

Device performance

Averaged data for DSSC devices prepared from the new dyes are collected in Table 3. Representative current-voltage ($J-V$) curves, measured at "one sun" after treatment with UV light,¹⁷ are shown in Fig. 1. The short circuit photocurrent

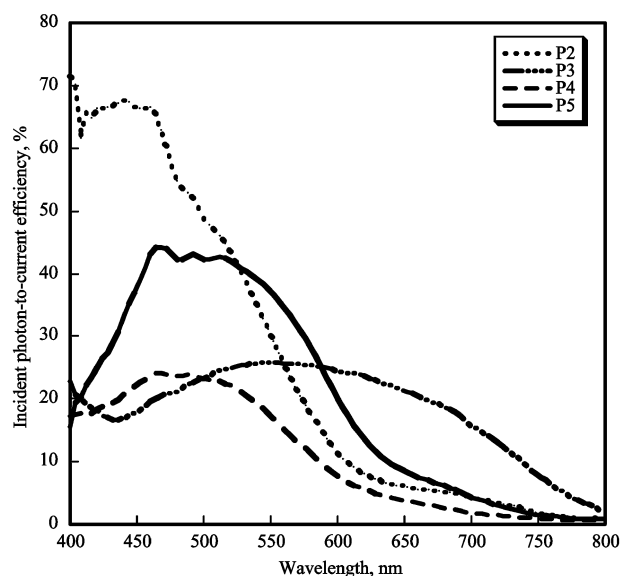
Table 3 Average solar cell parameters, from two measurements of each cell. Electrolyte conditions same as Fig. 2

Dye	Photocurrent/ mA cm ⁻²	Photovoltage/ V	Conversion efficiency/%
P1	4	-0.41	0.59
P2	8.9	-0.54	1.92
P3	9.7	-0.40	1.2
P4	4.5	-0.32	0.45
P5	9.8	-0.41	1.3
“N3” [Ru(4,4'-dcb- bpy) ₂ (NCS) ₂]	21	-0.59	4.4

**Fig. 1** *J-V* curve for P2, P3, and P5 illuminated at AM 1.5, “one sun”. Cells were UV treated and electrolyte was 0.5 M TBAI, 0.05 M I₂, 0.2 M 4-*tert*-butylpyridine in methoxypropionitrile.

(J_{sc}) and open circuit photovoltage (V_{oc}) are nearly identical for **P3** and **P5** in Fig. 1, and on average, these two dyes perform comparably (Table 3). In Fig. 1, the overall conversion efficiency (η), calculated from $J_{sc} \times V_{oc} \times FF/P_{in}$, where P_{in} is the incident power, is slightly higher for **P3** than for **P5** because of its better fill factor (FF). However, the best conversion efficiency is for 9-dioctylaminoperylene-3,4-dicarboxylic acid anhydride (**P2**), which has a smaller J_{sc} but larger V_{oc} than **P3** and **P5**. Accompanying incident photon-to-current efficiency (IPCE) data for the same three dyes, and also **P4**, are shown in Fig. 2. Maximum IPCE's are tabulated alongside the excited state potentials in Table 2. While **P2** has the greatest maximum quantum efficiency (IPCE near 70% at 440 nm), it collects a fairly narrow and high energy region of the spectrum, and absorbs very little beyond 600 nm. In contrast, the DSSC containing 9-dioctylamino-*N*-(acetic acid)perylene-3,4-dicarboximide (**P3**) has a very broad action spectrum. Thus, although it has a much lower IPCE maximum (~26% at 550 nm) than **P2**, its J_{sc} under white light illumination is greater because it makes better use of the lamp spectrum. **P5** has an action spectrum intermediate between **P2** and **P3** in both its spectral features and its IPCE maximum (~44% at 466 nm). **P4**, similar to the dyes used in our previous study,¹² is both a poor visible light collector and has a small IPCE maximum (~24% at 466 nm).

The oxidation potential of the perylene dyes (Table 1) are at least 400 mV positive of the I⁻/I₃⁻ couple (~0 V vs. Fc). The photocurrent in the DSSC device can be limited by slow

**Fig. 2** IPCE spectra for P2, P3, P4, and P5. Electrolyte conditions same as Fig. 2.

kinetics for dye regeneration if the driving force for iodide oxidation by the sensitizer is small.^{20,21} But we found little variation in J_{sc} for the I⁻ concentration range 0.25–1.0 M, showing that reduction of the oxidized dye by I⁻ is not rate limiting in this concentration range.

Discussion

We have synthetically tuned the electrochemical and light absorption properties of dyes based on the perylene chromophore, and thus significantly increased their efficiencies for solar conversion in the DSSC. More negative excited states contribute to improvements in their quantum efficiencies, and light absorption that is more coincident with the solar spectrum improves light collection in the devices. While all of the new perylenes make more efficient DSSC's than **P4**, there are some interesting trends that illustrate the contribution of both the quantum efficiency and the spectral distribution to the solar conversion efficiency.

The photocurrent and IPCE in the DSSC are affected by several processes in the cell; the steps specific to the sensitizing dye are injection, recombination of the injected electron with the dye, and re-reduction by I⁻. Re-reduction by I⁻ is not a limiting step for any of the perylene dyes, but injection efficiency and recombination may be highly variable amongst them. Some of the observed differences may be rationalized by an energetic argument. For example, although **P2**, **P3** and **P4** have very similar excited state energies in solution (Table 2), **P2**'s excited state shifts negatively when adsorbed onto TiO₂ (*vide supra*). The increased driving force for injection could explain its larger IPCE compared to **P3** and **P4** (Table 2). Likewise, **P5** has a more negative excited state potential and a larger IPCE than **P3** and **P4**. However, **P5** has a smaller IPCE than **P2**, which may indicate that in its adsorbed form, **P2** has a more negative excited state than **P5**.

Differences in quantum efficiencies between **P2** and **P3** or **P5** could also be related to differences in electronic coupling for the injection process. **P2** would be rigidly bound and its aromatic rings directly coupled to the TiO₂ through the linking carboxy group(s), whereas both **P3** and **P5** have flexible methylene units bridging the carboxy group and the chromophore. Both the flexibility of the dye on the surface and the weaker electronic coupling of the saturated spacer are likely to diminish injection efficiency. The parameters affecting

recombination between the injected electron and the dye are not well understood; both inverted region and orbital-based arguments have been invoked to explain the slow recombination in devices containing N3.² Durrant and coworkers showed that the recombination rate was insensitive to the nature of the sensitizer in a comparison of three sensitizers (N3, a zinc porphyrin and a free base porphyrin) with the same adsorbing linkage.²² However, the perylenes' different modes of surface binding (*i.e.*, **P2** vs. **P3**) could result in distinct recombination mechanisms. Clearly, time resolved measurements are required in order to quantify the injection and recombination kinetics.

It is interesting to note that dyes **P3** and **P5** were originally designed to determine if injection efficiency was dependent upon the excited state dipole. Both **P3** and **P5** have charge transfer character that directs the excited state electron density from the amine towards the imide end of the molecule. However, while **P3** would be attached at its electron-rich end to the TiO₂ surface, **P5** would be attached at its electron-poor end. Predicted differences—that **P3** would inject well and **P5** would not—are not apparent from the DSSC data. However, it is possible that the flexible linkages allow **P3** and **P5** to move about the surface and, by laying down flat, their adsorbed configurations are in fact similar.

These are the highest efficiencies yet reported for perylene sensitizers in the DSSC. The high quantum efficiency for **P2** compensates for an absorption spectrum that is not very good for solar conversion, and makes it an excellent sensitizer. While these dyes have much better solubility than the previous PTEDA-based generation, we have still not overcome problems of aggregation in solution and on the surface. For example, although **P1** and **P2** are nearly identical chromophores, **P2** is a much better sensitizer in the DSSC than **P1**. There was spectral evidence that **P1** was aggregated and this may explain its poor performance. We are continuing to explore the effects of aggregation and to pursue synthetic strategies that will yield truly non-aggregating dyes. **P3** is the most promising new sensitizer for solar conversion; it has a broad absorption spectrum that extends past 800 nm. Maximizing its overall IPCE would make its efficiency competitive with that of the N3 dye. If **P3** is limited by poor electronic communication, this may be alleviated by modifying the adsorbing linkage so that it provides greater coupling between the dye and the TiO₂.

Acknowledgements

We would like to thank the Director's Discretionary Research and Development program at NREL and the Office of Science, Division of Basic Energy Sciences, Chemical Sciences Division of the U.S. Department of Energy for funding this research.

References

- 1 B. O'Regan and M. Grätzel, *Nature*, 1991, **353**, 737.
- 2 A. Hagfeldt and M. Grätzel, *Chem. Rev.*, 1995, **95**, 49.
- 3 M. K. Nazeeruddin, M. Amirasr, P. Comte, J. R. Mackay, A. J. McQuillan, R. Houriet and M. Grätzel, *Langmuir*, 2000, **16**, 8525.
- 4 Y. Tachibana, J. E. Moser, M. Grätzel, D. R. Klug and J. R. Durrant, *J. Phys. Chem.*, 1996, **100**, 20056.
- 5 T. Trupke, P. Würfel and I. Uhlendorf, *J. Phys. Chem. B*, 2000, **104**, 11484.
- 6 J. van de Lagemaat, N.-G. Park and A. J. Frank, *J. Phys. Chem. B*, 2000, **104**, 2044.
- 7 B. A. Gregg, F. Pichot, S. Ferrere and C. L. Fields, *J. Phys. Chem. B*, 2001, **105**, 1422.
- 8 H. Langhals, *Heterocycles*, 1995, **40**, 477.
- 9 *Pigment Handbook*, ed. T. C. Patton, John Wiley & Sons, New York, 1973, vol. II.
- 10 K.-Y. Law, *Chem. Rev.*, 1993, **93**, 449.
- 11 B. A. Gregg and R. A. Cormier, *J. Am. Chem. Soc.*, 2001, **123**, 7959.
- 12 S. Ferrere, A. Zaban and B. A. Gregg, *J. Phys. Chem. B*, 1997, **101**, 4490.
- 13 H. Langhals, R. Ismael and O. Yürük, *Tetrahedron*, 2000, **56**, 5435.
- 14 L. Feiler, H. Langhals and K. Polborn, *Liebigs. Ann.*, 1995, 1229.
- 15 S. Ferrere, *Chem. Mater.*, 2000, **12**, 1083.
- 16 A. Zaban, S. Ferrere, J. Sprague and B. A. Gregg, *J. Phys. Chem. B*, 1997, **101**, 55.
- 17 S. Ferrere and B. A. Gregg, *J. Phys. Chem. B*, 2001, **105**, 7602.
- 18 D. Gosztola, M. P. Niemczyk and M. R. Wasielewski, *J. Am. Chem. Soc.*, 1998, **120**, 5118.
- 19 S. K. Lee, Y. Zu, A. Herrmann, Y. Geerts, K. Müllen and A. J. Bard, *J. Am. Chem. Soc.*, 1999, **121**, 3513.
- 20 D. Kuciauskas, M. S. Freund, H. B. Gray, J. R. Winkler and N. S. Lewis, *J. Phys. Chem. B*, 2001, **105**, 392.
- 21 M. Alebbi, C. A. Bigozzi, T. A. Heimer, G. M. Hasselmann and G. J. Meyer, *J. Phys. Chem. B*, 1998, **102**, 7577.
- 22 Y. Tachibana, S. A. Haque, I. P. Mercer, J. R. Durrant and D. R. Klug, *J. Phys. Chem. B*, 2000, **104**, 1198.